



## Group Coursework Submission Form

### Specialist Masters Programme

<b>Please list all names of group members:</b> (Surname, first name) 1. Kornakov, Marion 2. Musci, Edoardo 3. Patel, Prachin 4. Shah, Siddh		<b>GROUP NUMBER:</b> <div style="border: 1px solid black; padding: 5px; display: inline-block; margin-left: 10px;">3</div>	
<b>MSc in: Financial Mathematics, Quantitative Finance</b>			
<b>Module Code: SMM272</b>			
<b>Module Title: Risk Analysis</b>			
<b>Lecturer: Gianluca Fusai</b>		<b>Submission Date: 18/03/2024</b>	
<b>Declaration:</b> By submitting this work, we declare that this work is entirely our own except those parts duly identified and referenced in my submission. It complies with any specified word limits and the requirements and regulations detailed in the coursework instructions and any other relevant programme and module documentation. In submitting this work we acknowledge that we have read and understood the regulations and code regarding academic misconduct, including that relating to plagiarism, as specified in the Programme Handbook. We also acknowledge that this work will be subject to a variety of checks for academic misconduct.  We acknowledge that work submitted late without a granted extension will be subject to penalties, as outlined in the Programme Handbook. Penalties will be applied for a maximum of five days lateness, after which a mark of zero will be awarded.			
<b>Marker's Comments (if not being marked on-line):</b>			

**Deduction for Late Submission of assignment:**

**For Students:**  
 Once marked please refer to Moodle for your final coursework grade, including your Peer Assessment grade.

# Portfolio Risk Analysis

## Premises

The analysis has been performed on arbitrarily chosen assets, specified below. Given the provided dataset, the following caveats are important to be considered:

1. This study has been performed by using MATLAB-R2022b.
2. The Equally Weighted Portfolio is a combination of *Intel (INTC)*, *JP Morgan (JPM)*, *Alcoa Corporation (AA)*, *Procter and Gamble (PG)* and *Microsoft (MSFT)*. Stocks' prices have been obtained by scraping the Yahoo Finance webpage considering a time interval spanning from January 1<sup>st</sup>, 2014, to December 31<sup>st</sup>, 2023.
3. The risk-free interest rate considered to compute Sharpe Ratios was that of *US government Treasuries* between 5-year and 10-year bonds approximated to 4.315%.
4. For ease of computation, all the returns used in the calculations are logarithmic

## 1.1 Statistical Analysis

### 1.1.1 Introduction

The Classical Value at Risk methods assume constant volatility and a normally distributed return. A statistical analysis was conducted to determine if the chosen case study is affected by non-normality or autocorrelation, ensuring the reliability of subsequent VaR estimation.

### 1.1.2 Normality

The dataset presents a total of 2516 observations, and the Equally Weighted Portfolio returns have been constructed in the following way: let  $P_{i,j}$  be the  $j^{\text{th}}$  Stock price at date  $i$ , then:

$$R_{port_i} = \sum_{j=1}^5 \log \left( \frac{P_{i,j}}{P_{i-1,j}} \right) \cdot w_j \mid w_j = \frac{1}{j}$$

Typically, a daily return series fails to conform to normality, often displaying clustering around its mean, fat tails, and a pronounced peak. To examine the distribution of computed portfolio returns, a histogram has been plotted, depicting the empirical density of the data against a theoretical Gaussian distribution. This last probability density function has been calibrated with the same mean and variance extracted from the portfolio returns, respectively 0.004785 and 0.00020743.

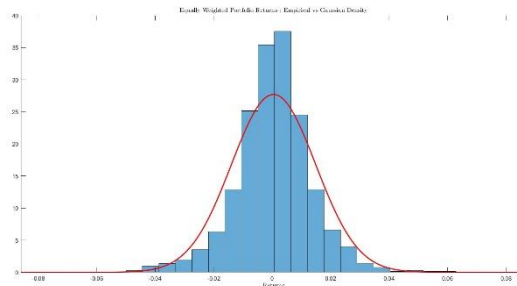


Figure 1

Confirming earlier expectations, this initial analysis reveals that the distribution of daily returns could deviate from normality. Specifically, the series demonstrates a high degree of symmetry around its mean, with a small and negative skewness value of approximately -0.53091. Moreover, its elevated excess Kurtosis of 16.484 indicates leptokurtic behaviour.

Addressing this departure from normality more effectively Figure 2 shows a zoomed perspective of the right and left tail of the above plot. It is expected to find fewer observations outside of the Theoretical Gaussian distribution, but instead, an occurrence of extreme values can be appreciated. Moreover, the minimum value recorded by the Equally weighted Portfolio is -0.1460 against the highest achieved of 0.1307, these features contribute to totalise 12 occurrences of negative outliers, which are more than 3 standard deviations away from the mean. Conversely, there are 13 observations classified as positive outliers, summing up to 25 excesses. This implies that the probability of such events is approximately 0.994%, equivalent to occurring roughly 2.4 times a year.

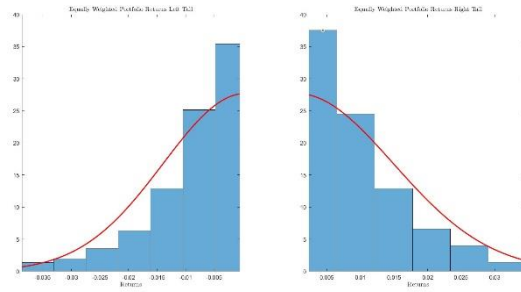


Figure 2

To delve deeper into this phenomenon, Figure 3 illustrates the count of observations within the 99.7% confidence interval, assuming the normality of returns.

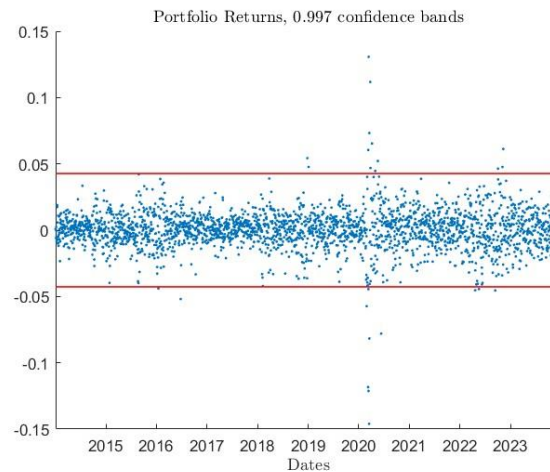


Figure 3

The observed frequency of observations falling within these intervals was 99.0060%, slightly below the expected 99.7%. This suggests that there are more observations outside this interval than anticipated under the Gaussian assumption. It is interesting to notice that under Gaussian distribution the probability of these extreme events to occur is about 1.07%, slightly higher than the empirical framework. The previous analysis suggests that the data deviate from a normal distribution, hence, to visually confirm this finding and statistically validate the departure from normality, two main tests were conducted. The first one is shown in Figure 4, illustrating the resulting QQ plot, which is instrumental in assessing whether two datasets originate from the same population and share a similar distribution. The plot was constructed by comparing a time series of normally distributed random variables, with the same mean and variance as the portfolio returns, against the actual series.

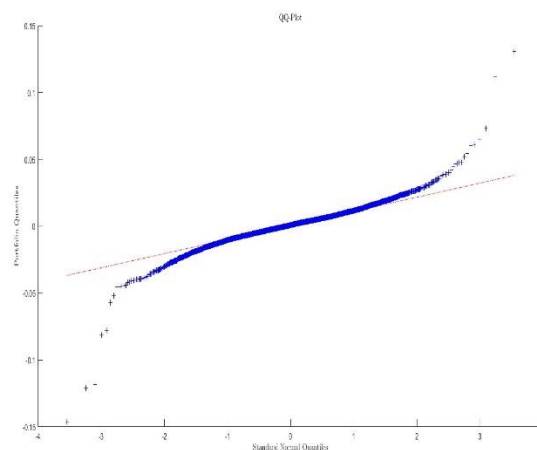


Figure 4

As evident from the plot, the distribution of the dataset exhibits symmetry around the mean, albeit displaying a slight negative skewness. Additionally, both tails appear thicker than those of a Gaussian distribution, indicative of high kurtosis. Notably, the upper quantiles of the returns surpass the 45° line, while the lower returns fall below it. The second statistical test performed to study the Normality of the dataset is the Jarque-Bera test. This tool assumes a null hypothesis, (with many observations) that the sample Skewness and the sample Excess Kurtosis follow a Gaussian.

distribution with mean 0 and Variance respectively 6 and 24. Additionally, since those two quantities are asymptotically independent the squares of their standardised forms can be added to obtain the test statistics as follows:

$$JB = \frac{T}{6}Sk_{\Delta}^2 + \frac{T}{24}(k_{\Delta} - 3)^2 \sim \chi_2^2$$

With:

- $T$ : Number of Observations;
- $Sk_{\Delta}^2$ : Squared Sample Skewness;
- $k_{\Delta}$ : Sample Kurtosis

This test asymptotically follows a Chi-square distribution with two degrees of freedom. In this instance, the critical value for a 95% confidence level was 5.9915, while the JB statistic yielded 19,172.60. Therefore, the assumption of normality can be rejected, and the normality of the data is discarded. Furthermore, the cumulative distribution function of a  $\chi_2^2$  computed at the JB test statistic level is 1, implying that the null hypothesis can be rejected in 100% of cases. To obtain a more accurate analysis of the Normality of returns over time, the Jarque Bera test has been performed over several periods, using a non-overlapping estimation reported in Table 1.

Window Size	Rejection rate	Mean Statistics
120	50%	62
200	75%	104
300	87.5%	214
450	100%	720
500	100%	839
800	100%	5162

Table 1

The results suggest that the Jarque-Bera test may not be a reliable indicator of normality, as the rejection rate decreases with smaller sample sizes. This implies a form of "size distortion" since the test relies on asymptotic validity, making it unsuitable for small sample sizes.

### 1.1.3 Autocorrelation

The second part of the statistical analysis focuses on assessing whether the series of returns exhibit independence and identical distribution. This examination is crucial because detecting autocorrelation within returns enables forecasting price variance, which, as mentioned earlier, is pivotal for Value at Risk assumptions, indeed, many VaR calculations methodologies operate under the assumption that return volatility remains constant or displays deterministic behaviour.

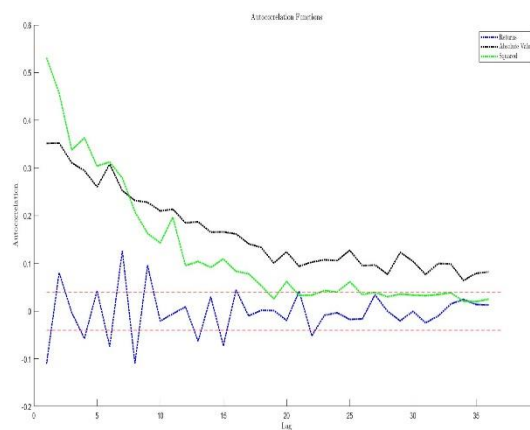


Figure 5

Figure 5 depicts the autocorrelation coefficients up to 36 lags, computed for 2 additional different versions of the original dataset, squared returns and absolute value returns such that:

$$\rho_k = \text{Corr}(J_{port_i}, J_{port_{i+k}}) \mid k = (1, 2 \dots 36)$$

$$J_{port_i} = (R_{port_i}, R_{port_i}^2, |R_{port_i}|)$$

Generally, if the return series was independent and identically distributed, the autocorrelation coefficient  $\rho_k \sim N\left(-\frac{1}{T}, \frac{1}{T}\right)$  so that the 95% confidence intervals can be computed as:

$$\alpha_{1,2} = \pm \frac{1}{T} + 2 \cdot \frac{1}{\sqrt{T}}$$

With 2 indicating the number of standard deviations from the mean. In this case, the returns do not exhibit statistically significant autocorrelation, with values ranging between 0.1261 and -0.1108,  $\rho_k$  fluctuates considerably for the first 10 lags and gradually stabilize thereafter. Whereas high significant levels of autocorrelation are appreciable for  $R_{port_i}^2$  and  $|R_{port_i}|$ , so can be concluded that the variance of returns is predictable. To enhance the analysis of autocorrelation, two additional statistical tests have been employed. The Portmanteau Q-statistic of the Box-Pierce test assumes the null hypothesis of no autocorrelation. In all cases, the test statistics yielded higher values than those expected from a chi-square distribution with 36 degrees of freedom  $\varphi(x_{36}^2) = 50.9985$  suggesting a correlation among returns. For comprehensive evaluation, the Ljung-Box statistic was utilized as a proxy for the aforementioned test. The results are presented in the table below, affirming the previous findings.

Target	$H_0$	$p$	Statistics	Z
$R_{port_i}$	reject	0	223.12	50.998
$R_{port_i}^2$	reject	0	3063.3	50.998
$ R_{port_i} $	reject	0	3074.6	50.998

Table 2

## 1.2 Value at Risk

### 1.2.1 Methodology

The estimation of Value at Risk was conducted using a rolling window size of 6 months. Given the data's nature, the annual timeframe comprises 250 observations, resulting in approximately 20 observations per month. The rolling window initiated its first iteration from January 2014 to July 2014, employing an overlapping method where: size has been set equal to 120, the window specified as  $window_\Delta: [R_{port_i}, R_{port_{i+120-1}}]$ ,  $i \in [1, 2515]$  with confidence intervals  $\alpha_j: [0.01, 0.99]$ ,  $j \in [1, 99]$  with  $\Delta$  indicating the number of iterations equal to  $T - size + 1$  and the VaR has been estimated by following three different methodologies:

**Parametric VaR (PV):** assuming Normality of returns is respected, the *window-sample* mean and variance have been estimated, computing the critical value relative to the  $\alpha_j$ -th confidence interval as follows:

$$VaR_{Parametric_t} = -(\mu_\Delta + \sigma_\Delta \Phi^{-1}(1 - \alpha_j))$$

**Non-Parametric VaR (NPV):** uses actual historical data, and makes no hypothesis about the distribution of the data, it has been obtained by sorting the  $\Delta$  as a non-decreasing sequence, computing:

$$c = (1 - \alpha_j); VaR_{Non Parametric_t} = -p^c(\Delta)$$

**Monte Carlo VaR (MCV):** Future data have been generated, calibrating the model on each  $\Delta$  to obtain a simulated distribution of data:

$$k_t = \mu_\Delta \cdot size - \frac{(\sigma_\Delta \sqrt{size})^2}{2}$$

$$VaR_{Monte Carlo} = p^c \left( X_s \sqrt{\frac{1}{250} \sigma_\Delta \sqrt{size}} + k_t \frac{1}{250} \right)$$

With  $X_s$  a series of random numbers drawn from a standard Normal distribution, such that  $X_s \sim N(0,1)$ ,  $s = 500$ ;

Figure 6 illustrates the varying behaviour of the three different types of Value at Risk (VaR) as confidence intervals change. While PV and NPV exhibit similar patterns, MCV appears less cautious, attributing higher VaR values to smaller confidence intervals and vice versa for higher confidence levels. This tendency towards overestimation suggests the need for further analysis to address this discrepancy.

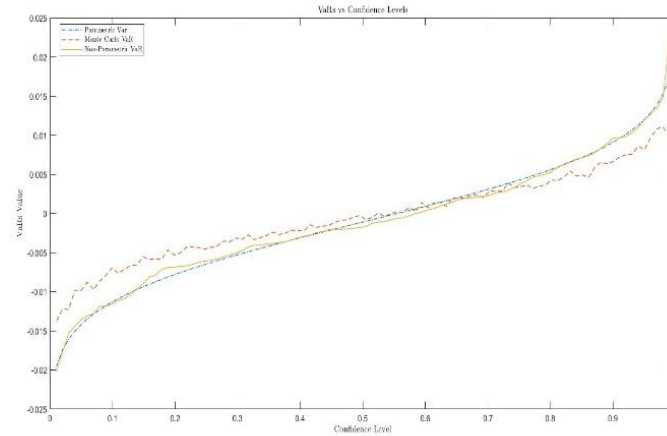


Figure 6

The graph below illustrates the temporal evolution of PV, NPV, and MCV computed at a 90% confidence interval. Notably, PV displays a less stable trend over time, characterized by higher fluctuations compared to its counterparts. Furthermore, a consistent tendency towards overestimation is evident throughout the entire sample period and particularly during periods of high volatility. PV estimates VaR to be approximately 28.5% higher than NPV during such volatile clusters.

Conversely, both MCV and NPV demonstrate comparatively smaller variability over time, with less pronounced peaks and troughs. The previous observations regarding the less cautious estimations of MCV are further validated by its consistently lower value. This discrepancy may stem from the differing complexities of the models employed to estimate VaR. MCV, for instance, utilizes normal random numbers in its estimation process, potentially rendering it less sensitive to rapid fluctuations in sample mean and variance. In contrast, PV relies heavily on these factors.

Regarding NPV, it appears to behave as a middle ground between its two counterparts. It is important to note that, despite temporal variations, all VaR calculation methods maintain an acceptable level of risk coverage, as affirmed by retrospective analysis of historical data.

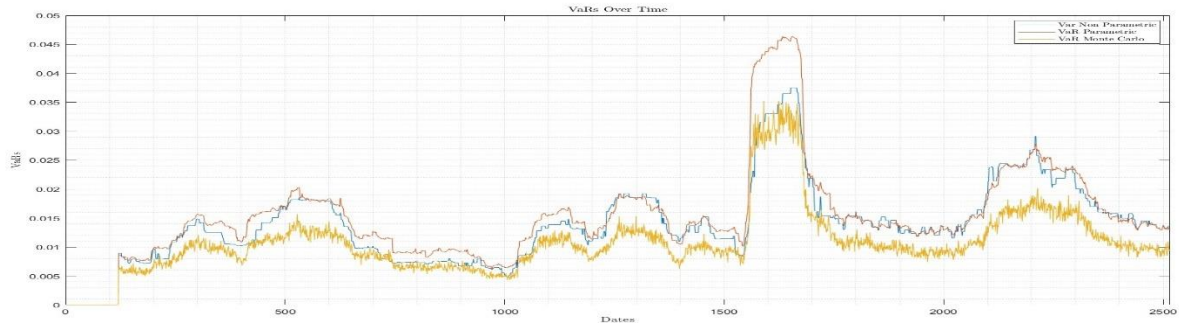


Figure 7

### 1.2.3 Violations Analysis

Figure 8 plots the results of the analysis of a 90% VaR level, for a sample period of high volatility, between 2019 and 2022, taking in consideration the following definition of Violation:  $V_{ij} = R_{port_i} \leq VaR_{ij}$  with  $j$ , the relative confidence interval chosen.

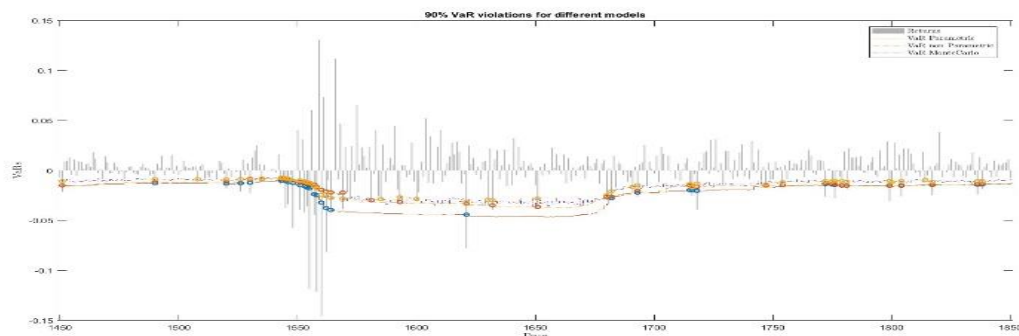


Figure 8

Hence, a VaR failure occurs when returns exhibit a negative VaR. Closer examination around the selected dates reveals significant turbulence in returns. Starting from 2019 onwards, the PV closely and accurately tracks the return trend. As a result, PV exhibits fewer VaR violations (blue circles) compared to the MCV approach (yellow circles) or the NPV method (red circles). As noticed before, MCV and NPV tend to frequently miss capturing immediate price return changes, closely trailing during clusters of volatility.

Expectations on number of Violations recorded by each model decrease with the confidence interval under Normality assumption, indeed given a certain  $\alpha_j$ , the expected number of violations is computed as:

$$E(V_j) = \alpha_j T$$

The bar plot depicted in Figure 9 illustrates how the number of violations varies across different VaR levels, presenting the expected number of violations as a proxy for the models' performance. At smaller confidence intervals, the observed number of violations is notably high, as anticipated. It is intriguing to observe that as accuracy increases, the MCV model tends to accumulate more violations than both PV and NPV. The NPV achieves the optimal balance of violations that align with expectations, matching the expected number of violations in two instances,  $\alpha_j=0.90$  and  $\alpha_j=0.99$ .

Nevertheless, it is crucial to acknowledge that even at higher confidence levels, significant violations may occur, indicating potential inaccuracies in capturing extreme risks by the model. This graph offers a valuable visualization of the VaR model's effectiveness and its inherent limitations in identifying and mitigating market risks.

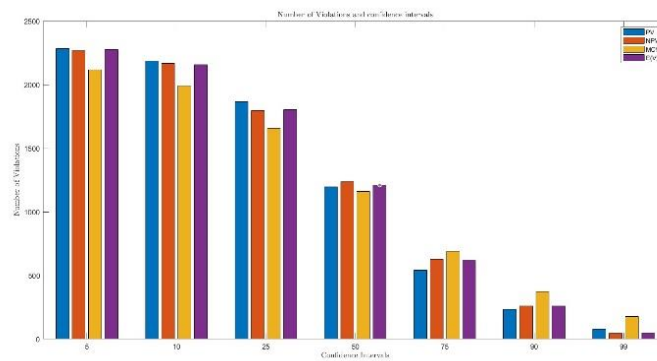


Figure 9

### 1.2.4 Kupiec Test

The Kupiec test is a likelihood ratio test used to assess if the proportion of failures (number of failures divided by number of observations) is consistent with the VaR confidence level. Its null hypothesis assumes that the observed failure rate  $p$  is equal to the failure rate suggested by the confidence interval. The table below shows the results obtained when running this test at a 95% level of significance for all simulated back test models.

	PV	NPV	MCV	$\alpha_j$
$V_j$	220	252	352	
<b>LRatioPOF</b>	1.8266	0.7024	62.9558	0.90
<b>Decision</b>	accept	accept	reject	
$V_j$	53	26	144	
<b>LRatioPOF</b>	26.4310	0.1707	271.6018	0.99
<b>Decision</b>	reject	accept	reject	

Table 3

The Parametric approach used to estimate PV fails to accept the null at a 99% confidence interval but is considered accurate for a 90% level. In both cases, the NPV accepts the null, as an additional confirmation the following ratio can be computed:  $\frac{V_{jNPV}}{T} \sim 1\%$ , different story for the MCV, which has been discarded in both cases.



## 1.3 Stress Testing

### 1.3.1 Clusters of Violations

To detect eventual clusters of Volatility an additional time series has been computed, first recognizing if the VaR estimation has been violated and then computing the actual difference between the predicted VaR at 99% confidence level and the actual returns, following the formula:

$$\zeta_i = \text{Min} \{R_{port_i} - (-VaR_k^{0.01}), 0\} / \sigma_{R_{port_i}}$$

In this way an array of differences and zeros has been obtained building the following plots:

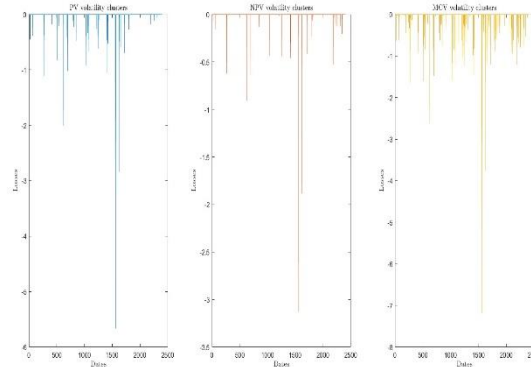


Figure 10

From Figure 10 is clear that violations cluster for MCV values, indeed occurring in a very short time span and often in adjacent days. To test for violations significance, the violation series must be stationary and independent, therefore, the main objective is to find a model with occasional violations distributed uniformly across time, because the closer the violations, the higher the risk of “default,” in this sense the models that respect this characteristic are the PV and the NPV. It is interesting to notice how clusters of Volatility happen during Covid-Lockdown Pandemic period and are not addressed completely by none of the model, this might be a sign of Model misspecification.

### 1.3.2 Stress Testing-CC test

All the tests that have been implemented use the “Hit Sequence,” which is takes value of 0 if the VaRs have not been violated and 1 if the violation has occurred. The test chosen to complement the violations clustering analysis is the Conditional Coverage test (CC), which assess the independence of failures on consecutive time periods. In particular it tests simultaneously if VaR violations are independent, and the average number of violations is correct. The Table reported below shows the results of this test for two different VaR levels:

	PV	NPV	MCV	$\alpha_j$
$V_j$	220	252	352	
<b>LRatioCC</b>	14.5077	10.6706	59.0736	0.90
<b>CC</b>	reject	reject	reject	
$V_j$	53	26	144	
<b>LRatioCC</b>	37.3032	9.5155	288.9708	0.99
<b>CC</b>	reject	reject	reject	

Table 4

### 1.3.2 Stress Testing – Distribution Testing

In this phase of stress testing, rather than focusing on specific risk metrics derived from return distributions, the analysis backtests the entire return distribution. Specifically, assuming that the risk model generates a cumulative distribution function for returns, we calculate the model's probability of observing a return below the actual value. This calculation is performed as follows:

$$p_i = \Phi(R_{port_i})$$

Once the transformed probability time series is obtained, it can be visualized as a histogram. Ideally, it should exhibit a uniform distribution, represented by a  $p_i \sim U(0,1)$  variable. However, as observed in the figure below, systematic deviations from the expected flat line occur. This suggest that the model's distribution is mis-specified.



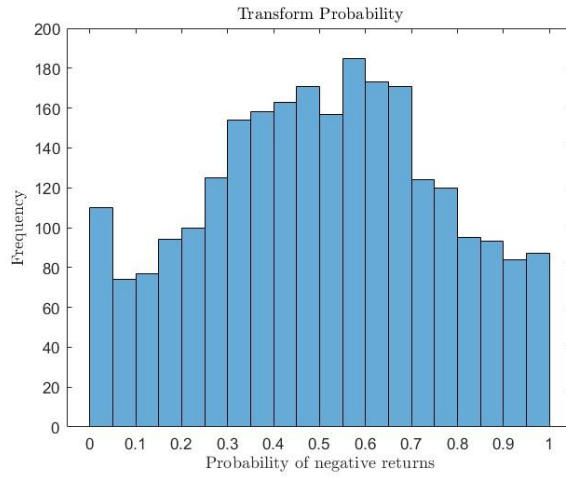


Figure 11

To proceed with the distribution test  $p_i$  is transformed into  $z_i \sim N(0,1)$ , by taking  $\Phi^{-1}(\Phi(R_{port_i}))$ , the figure below reports the histogram computed for the new Normal standard random variable, and as noticeable it does not follow a Normal distribution, also previous tests have been run to confirm this hypothesis, like the Jarque Bera which rejected the Normality of the Variable.

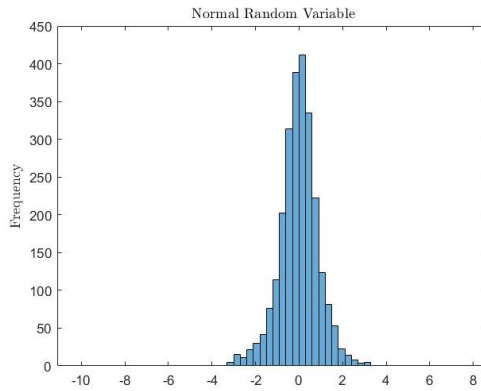


Figure 12

These graphic tests are obviously not enough to assess if the distribution chosen is the correct, hence a likelihood ratio test has been performed on  $z_i$ , first evaluating the model:

$$\tilde{z}_i = \beta_0 + \beta_1' X_t + \sigma z_i$$

$X_t$  are the Portfolio returns and  $\sigma$  its standard deviation, this model allowed the estimation of  $\widetilde{\beta}_0, \widetilde{\beta}_1'$  and  $\widetilde{\sigma}^2$ , with  $\widetilde{\sigma}^2$  the error variance, hence computing:

$$L_1 = -\frac{T}{2} \ln(2\pi) - \frac{T}{2} \ln(\widetilde{\sigma}^2); L_2 = \sum_{i=1}^T \frac{(\tilde{z}_i - \widetilde{\beta}_0 - \widetilde{\beta}_1' X_t)^2}{2\widetilde{\sigma}^2}$$

And obtaining the likelihood for the model:

$$\ln L(\widetilde{\beta}_0, \widetilde{\beta}_1', \widetilde{\sigma}^2) = L_1 - L_2$$

To find the Likelihood ratio test for correct risk model the above computation has been repeated, for  $\ln L(0,0,1)$  obtaining:

$$LR = -2(\ln L(0,0,1) - \ln L(\widetilde{\beta}_0, \widetilde{\beta}_1', \widetilde{\sigma}^2)) \sim \chi_4^2$$

Which follows a chi-square distribution with same number of elements of  $\widetilde{\beta}_1' + 2$ . In this case study the null hypothesis that

$$H_0: p_i \sim i.i.d \text{ Uniform}(0,1)$$

has been rejected, because of the large size of the LR ratio test obtained, this confirms what has been tested graphically in the above paragraph, concluding that the Model is misspecified and it does not follow a  $N(\mu_\Delta, \sigma_\Delta)$ .

## 2.1 Risk Parity Portfolio

### 2.2.1 Definitions

In the formulation of a *risk parity portfolio*, an essential aspect lies in the determination of component Value at Risk (VaR). Component VaR (CVaR) serves as a pivotal metric in quantifying risk contribution, drawing upon the attributes of individual portfolio components and their respective weights, signifying the proportion invested within the portfolio. As articulated, CVaR can be understood as "*A partition of the portfolio VaR that indicates how much the portfolio VaR would change approximately if the given component was deleted*" (Jorion, 2007).

To effectively compute CVaR, it becomes imperative to incorporate Marginal VaR (MVaR), which encapsulates sensitivity. MVaR defines the change in marginal risk concerning alterations in the allocation weights within the portfolio, accounting for the covariance between the asset in question and the portfolio as a whole. In essence, MVaR can be conceptualized as "*The change in portfolio VAR resulting from taking an additional dollar of exposure to a given component.*" (Jorion, 2007).

### 2.2.2 Methodology

The MVaR and CVaR are computed as follows:

$$MVaR = \frac{-z(1 - \alpha) * cov(returns) * weights}{(weights' * cov(returns) * weights)^{0.5}}$$

where z: standard normal distribution inverse of the confidence interval  $(1 - \alpha)$ .

$$CVar = weights * MVaR$$

The impact of the marginal contribution of risk can be assessed by the sensitivity of the portfolio volatility to a small change in the weights the following relationship:

$$\frac{\partial \sigma(portfolio)}{\partial w} = \frac{cov(Ri, Rp)}{\sigma(portfolio)}$$

Through exploiting these relationships, the risk-parity portfolio is built by optimising the weights through a minimising procedure of the dispersion, the standard deviation of the individual CVaRs, using the parametric variance-covariance approach.

### 2.2.3 Analysis

Within our empirical study, utilising the first half of the stock data from the previous analysis we are evaluating the MVaR, CVaR and the %CVaR contribution of an equally weighted portfolio and the risk-parity portfolio, with the following weights obtained.

	Weights	MVaR	CVaR	CVaR\%
INTC	0.2	0.01888	0.0037761	0.20734
JPM	0.2	0.015504	0.0031007	0.17026
AA	0.2	0.031309	0.0062618	0.34383
PG	0.2	0.0076544	0.0015309	0.08406
MSFT	0.2	0.017711	0.0035422	0.1945

Table 5

	Weights	MVaR	CVaR	CVaR\%
INTC	0.16946	0.018925	0.0032071	0.2
JPM	0.20163	0.015906	0.0032071	0.2
AA	0.11986	0.026758	0.0032071	0.2
PG	0.33279	0.009637	0.0032071	0.2
MSFT	0.17625	0.018196	0.0032071	0.2

Table 6

In the provided tables, Table 5 and 6, it is evident that in an equally weighted portfolio across various stocks, AA exhibits the highest contribution towards the Value at Risk (VaR), accounting for approximately 34.38%, followed by INTC at 20.73%. Conversely, PG demonstrates the smallest risk contribution at approximately 8.41%. This analysis suggests that AA represents the riskiest asset within the portfolio, while PG stands as the least risky. The claim of AA being the riskiest stock within this portfolio is supported by the weight allocated to AA after the minimising procedure of the CVaR. Specifically, the proportion invested in AA diminishes from 20% to 11.99 whereas the allocation to PG, the less risky asset, increases from 20% to 33.28%. This change in weights contributes therefore to a less risky portfolio, taking advantage of diversification. While it is noteworthy, that the risk concentration of the CVaR is evenly distributed throughout the stocks, within the risk parity portfolio. To expand our analysis on the Component VaR and its sensitivity

with regard to changes in the weight, in addition to the risk parity and equally weighted portfolio, we have generated a “minimum variance portfolio” which optimises the portfolio proportionality, i.e. weights with regard to minimising the variance of the portfolio. The effect on the proportionality of the CVaR/% of the 3 portfolios can be observed in the Figure 13.

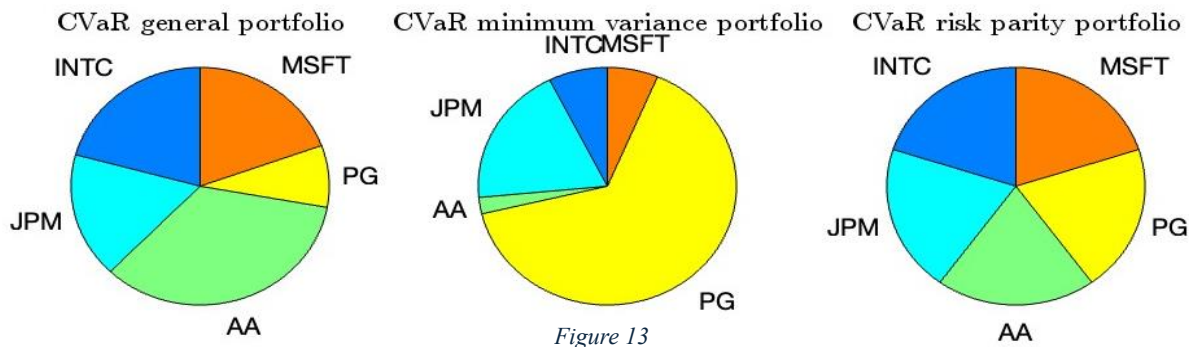


Figure 13

Upon visual examination of Figure 13, supports the above claim that the largest value at risk proportion comes from AA and the smallest from PG in the "general portfolio," where we assume equal amounts invested in all assets. The second pie provides more evidence for this claim, as it shows that by minimising portfolio variance, the highest proportional investment goes into PG and the lowest into AA (as indicated by the CVaR/%). As a result, increasing your investment in the least hazardous asset will reduce your portfolio's variance and respective CVaR. Lastly, by assigning the weights in accordance with Table 6, the CVaR of the risk parity portfolio shown in the third pie emphasises the even distribution of the component value at risk.

Next, we estimated the cumulative returns using the second half of the data, as shown in figure 14, by using the optimised weights found in the risk parity portfolio and considering the equally weighted portfolio. Towards the beginning and end of the sample, it is evident that the risk parity portfolio's return outperforms the equally weighted portfolio's return. On the other hand, the returns can be thought of as nearly equal in the middle of the sample.

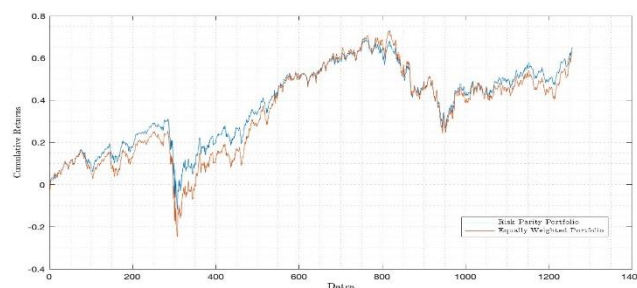


Figure 14

To further measure the performance of the portfolios we consider the Sharpe Ratio Index and the Maximum Drawdown. The Sharpe ratio index compares the return of the portfolio with its respective risk to the risk-free rate of return, which can be considered a proxy for the return of a risk-free asset. It is a mathematical expression which allows for insight regarding the “reward-to-variability ratio,” hence it allows us to evaluate whether the excess return of the investment is appropriate given its respective risk level. In essence the higher the Sharpe ratio the better is the return considering the respective volatility. The Sharpe Ratio is computed as follows:

$$\text{Sharpe Ratio} = \frac{\text{Expected Return (portfolio)} - \text{Risk free rate}}{\text{Standard Deviation (portfolio)}}$$

Sharpe_Equally_Weighted	Sharpe_Risk_Parity
-2.4959	-2.8454

Table 6

Within our empirical study we have utilised the US government treasury rate as the risk-free asset rate which lies at approximately 4.315%. As the equally weighted portfolio distributes the weights invested into the assets equally, its negative Sharpe ratio -2.4959 highlights the portfolios inability to generate positive excess returns. This implies that the portfolio's returns are insufficient given the amount of respective risk. The underperformance of the excess returns might be a result of unsuccessful diversification, bad asset selection, or large exposure to high-risk assets.

By comparison, the risk parity portfolio, which aims to be balancing risk across assets, has an even lower Sharpe ratio of -2.8454. This suggests that risk has not been well diversified, and the return generation has not been successful in the risk parity portfolio, so that excess returns would be appropriate given its risk level. Regarding the risk parity portfolio's Sharpe ratio being lower, it highlights that the weight allocation with regard to its risk is even worse than the equally weighted one. Therefore, the poor risk allocation decisions can be due to miscalculations and underestimation of the asset's volatilities.

Moving forward we examined the maximum drawdown, which is a fundamental concept in portfolio risk assessment, it is a key metric for investors aiming to analyse the possible downside exposure of their investments. It captures the extent and exposure of losses under unfavourable market conditions by showing the largest drop in value from peak to trough that a portfolio experiences over a given time period. This indicator is useful as it provides an overall perspective on the stock performance, through providing assessing the portfolio's resilience and risk tolerance, taking the volatile price fluctuations into account over time. The maximum drawdown helps investors understand how volatile their investments are helps in predicting the possible effects of market downturns on their portfolio value. This is achieved through putting a number on the worst-case scenario in terms of loss magnitude. Hence, the analysis of

maximum drawdown can aid in the implementation of risk management strategies, which allows investors to adjust their investment approach through aligning their risk tolerance with their return goals. By minimising the maximum drawdown investors can protect the value of their investment.

Mathematically the maximum drawdown (MDD) can be calculated as:

$$MDD = \frac{\text{Trough Value} - \text{Peak Value}}{\text{Peak Value}}$$

Considering this formula the embedded MATLAB function “*maxdrawdown*” considers the entirety of the dataset. Within our analysis we have computed the maximum drawdown taking into account the prices for the first half of the dataset, the prices of an equally weighted portfolio and the risk parity portfolio. The equally weighted portfolio's maximum drawdown is 0.32731, which shows the biggest range of percentage drop from a peak to a trough over a given time period. This amount of maximum drawdown shows how susceptible the portfolio is to large losses. This means that in the worst or most volatile circumstances investors would have experience a 32.73% loss in the value of their investments.

Max_Drawdown_Equally_Weighted	Max_Drawdown_Risk_Parity
0.32731	0.31127

Table 7

Such a drawdown shows how vulnerable the portfolio is to unfavourable market conditions and could potentially cause a significant loss of capital. High exposure to underperforming assets or industries, poor risk management procedures, or increased market volatility that adversely affects portfolio performance are all potential causes of this drawdown.

The risk parity portfolio shows a marginally lower maximum drawdown of 0.31127, which suggests that a relatively smaller loss in portfolio value would occur under unfavourable market circumstances. This drawdown level indicates a comparatively more robust portfolio structure, which might be due to the risk being equally distributed across the 5 assets, such that investors witness a roughly 31.13% drop in portfolio value at its lowest point. Hence, the risk parity strategy's emphasis on distributing risk across assets, may have helped in the reduction of losses during volatile market conditions. Because the drawdown was less than that of the equally weighted portfolio, it can be assumed that the weight allocation was better in regard to the risk level. Regardless, the drawdown is still a significant cause for concern, as a loss of above 30% in portfolio value in stressed market conditions is not favourable.

To summarise, both portfolios indicated significant losses, but the risk parity portfolio shows marginally better response to volatile markets than the equally weighted portfolio. However, the amounts of the maximum drawdown in both situations highlight the importance of risk management and effective diversification, to lessen the effects of unpredictable markets.

## 2.2.4 VaRs

Proceeding our analysis of the risk parity portfolio, we estimated the Value at Risk using three approaches: Parametric, Non-parametric, and with a rolling window (referred to as the 'loop'), all conducted at a 95% confidence level. These techniques differ in their level of sophistication and assumptions about portfolio return distribution. The parametric

method uses past data in the VaR estimation by assuming a probability distribution, like the Gaussian distribution. While the non-parametric technique offers more flexibility, it may require bigger datasets for more exact and successful estimates since it does not use any assumptions on the distribution and instead computes the VaR directly from gathered data. Finally, by continuously updating VaR estimates using a rolling window of the historical data, that technique offers a dynamic evaluation that more accurately captures changing market conditions, as opposed to the parametric and non-parametric approaches as it does assume a singular, stationary value for the Value at Risk.

violations_Parametric	violations_Non_Parametric	Parametric_VaR_violations_loop
40	8	12

Table 8

As part of our analysis, we assess VaR violations, which occur when the portfolio returns exceed the estimated VaR values. These violations reveal potential deficiencies in risk management plans or VaR metrics and act as markers of unforeseen losses that exceed projected risk thresholds.

The amount of VaR violations for the risk parity portfolio varied depending on the estimating method we used, according to our analysis. In particular, the parametric method found about 40 violations and 8 in the non-parametric, indicating that the risk may have been underestimated by the VaR. Given the Gaussian distribution and non-parametric methods the expected violations should be higher, approximately 63 for the given sample size, which is favourable in terms risk evaluation.

The rolling window technique, which is dynamic in nature, found 12 violations and revealed information about the risk exposure of the portfolio over time. This strategy still identified situations where the portfolio's real losses exceeded the predicted risk levels, but it did so in a way that was more sensitive to shifting market conditions. These results highlight the significance of effective risk management procedures and the use of suitable VaR calculation techniques for building investment portfolios.

The examination of VaR violations has important future implications for managing and building risk parity portfolios. VaR violations indicate areas where risk allocation techniques need to be improved, even though the risk parity portfolio's goal is to balance risk among assets. It is advisable for investors to thoroughly evaluate the advantages and disadvantages of various VaR assessment methods and modify their risk management strategies accordingly.

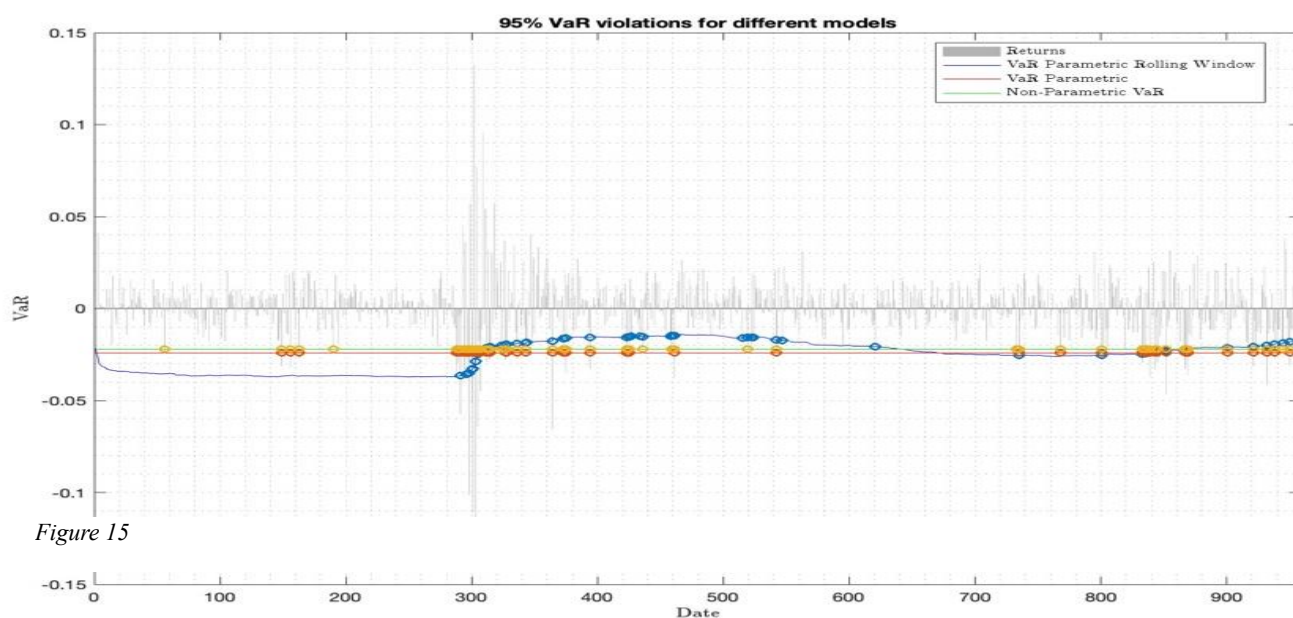


Figure 15

To summarise, the in-depth investigation of VaR estimates and violations offers important new perspectives on how well risk management techniques work inside the risk parity portfolio. Investors may work to optimise the risk-return profile of their portfolios and more successfully accomplish their investing goals over time by utilising these insights and improving risk allocation technique.



## 3.1 VaR of a Bond

### 3.1.1 Methodology

The procedure for calculating the yield to maturity (YTM) of the bond is by determining the interest rate at which the bond price is equal to the current bond price of \$99. Since the bond price is lesser than its face value of \$100 suggesting that the YTM must be greater than the coupon rate of 3% thus analytically solving for the YTM using mathematical techniques such as root finding. In this case, the equation representing the present value of the bond's future cash flows is set up, and then a symbolic solver is employed to find the interest rate that satisfies the equation below.

$$\sum_{i=1}^T \left( \frac{C}{(1 + YTM)^i} \right) + \left( \frac{FV}{(1 + YTM)^T} \right) = P_0$$

With:

- $C$ : Coupon
- $YTM$ : Yield to Maturity
- $FV$ : Face Value
- $P_0$ : Current Bond Price
- $T$ : Maturity

This resulted in the YTM being equal to 3.22%. It represents the annualized return an investor can expect to earn if they purchase the bond at its current market price and hold it until maturity, assuming reinvestment of coupon payments at the same YTM. This metric is crucial for investors as it provides insights into the attractiveness of the bond as an investment opportunity relative to other options available in the market. Similarly, to estimate the probability of 10% decline in the bond price within a 30-day period, one must compute the YTM at which the bond price is 90% of its current price. In this case the bond price is \$90 at 5.56% YTM. Now to assess the likelihood of this scenario occurring, a probability calculation is performed. As the daily variations in YTM follow independent and identical distributions (i.i.d) Gaussian random variables with mean 0 and standard deviation of 0.006 one can employ the normal cumulative distribution function to estimate the probability that the YTM exceeds the computed value for the scenario. Since the bond price decline would be higher if the YTM does exceed the computed amount. Thereby the resulting probability of 4.54% represents the likelihood of observing a YTM that would yield to the anticipated 10% decline in the bond's price over the 30 days. Understanding this probability is important for investors as it provides insights into the risk associated with holding the bond over the short-term horizon. It allows investors to assess the probability of significant price declines and make informed decisions based on their risk tolerance and market expectations.

One of the approaches of computing the value at risk (VaR) for a coupon paying bond is using the Exact Formula. Bond prices can be calculated using a closed-form formula such equation, and the pricing formula is a monotonic function of the underlying risk factor (change in yields) thus enabling one to obtain a simple VaR formula:

$$VaR_{\alpha}^t = Z_{1-\alpha} \times \sigma_{dy} \times \sqrt{t} \times P_0$$

With:

- $Z_{1-\alpha}$ : Z-score at  $\alpha\%$  confidence level equal to  $\Phi^{-1}(\alpha)$
- $\Phi$ : CdF of Gaussian Distribution
- $\sigma_{dy}$ : Daily standard Deviation of change in YTM
- $t$ : Horizon

In the exact formula approach, VaR is computed directly using the formula based on the historical volatility (standard deviation) of the YTM movements. This method assumes a normal distribution of returns and calculates the potential loss at a specified confidence level (typically 99%) over different time horizons. In the case of bonds, the monotonic function is decreasing since the bond prices to yield to maturity are negatively related and is convex. Therefore, a gain in the risk factor (YTM) will imply a loss on the long bond position. However, there are multiple limitations to this approach. It especially requires the price of the asset to be computable easily and the dependence the risk factor to have. a monotonic function. This can be aided by using the Taylor's approximation where it incorporates the delta of the bond in the pricing as below:

$$\frac{\Delta P}{P} = -Duration \times \frac{\Delta_{YTM}}{(1 + YTM)}$$

This modifies the Exact Formula as follows:

$$VaR_{\alpha}^t = Z_{1-\alpha} \times \sigma_{dy} \times \sqrt{t} \times P1$$

Where:

$$P1 = P0 + P0 \times \Delta_{P0} \times \frac{\Delta_{YTM}}{(1 + YTM)}$$

$\Delta_{P0} = \text{Duration of Coupon Bond equals}$

$$\frac{\sum_{i=1}^T \left( \frac{C \times i}{(1 + YTM)^i} \right) + \left( \frac{FV \times T}{(1 + YTM)^T} \right)}{P0}$$

And

$$\Delta_y = \text{Change in YTM}$$

The delta approximation method utilizes the bond's duration, a measure of its price sensitivity to changes in interest rates. By estimating the change in bond price resulting from a small change in interest rates (delta), VaR is computed. This method provides a more refined estimate compared to the exact formula by considering the bond's specific characteristics. Although there are still drawbacks in estimating the change in bond prices based on just duration. As it assumes that the yield curve shifts in a parallel manner, meaning that the yields across all maturities change the same amount. In reality, yield curve shifts can be non-parallel, with different maturities experiencing different changes in yield. This can lead to inaccuracies in the estimated price change using duration. This suggests that Duration is a linear measure and does not take into account the convex relationship between bond prices and yields. Therefore, the new and better approach is the delta-gamma approximation via Taylor's approximation as it incorporates the convexity of the bond. Convexity i.e. gamma captures the curvature of the bond's price yield, providing additional information which offers a more accurate estimate of VaR, particularly for larger changes in interest rates. Thus, the second order Taylor's approximation and exact formula changes to:

$$\frac{\Delta P}{P} = -\text{Duration} \times \frac{\Delta_{YTM}}{(1 + YTM)} + \frac{1}{2} \times \text{Convexity} \times \Delta_{YTM}^2$$

$$VaR_{\alpha}^t = Z_{1-\alpha} \times \sigma_{dy} \times \sqrt{t} \times P2$$

where P2 is

$$P0 + P0 \left( \Delta_{P0} \times \frac{\Delta_{YTM}}{(1 + YTM)} + \frac{1}{2} \times \Gamma_Y \times \Delta_{YTM}^2 \right)$$

Hence,

$\Gamma_Y = \text{Convexity of Coupon Bond:}$

$$\frac{\sum_{i=1}^T \left( \frac{C \times i(i+1)}{(1 + YTM)^i} \right) + \left( \frac{FV \times T(T+1)}{(1 + YTM)^T} \right)}{P0 \times (1 + YTM)^2}$$

Overall, these methods allow investors to quantify the potential downside risk associated with holding the bond under different scenarios of interest rate movements. The results provide valuable insights into the potential losses investors may incur over various time periods, aiding in risk management and portfolio decision-making. Since the greeks for the bonds have analytical formulas it's relatively straightforward to update the exact formula however, for other more complex derivatives like European calls and puts the greeks are found by their numerical approximations. Using the above 3 mentioned methods one obtains the following VaR values for the bond at hand for horizons varying from 1 to 90 days:



Days	Exact Formula	Delta Approximation	Delta Gamma Approximation
1	-1.3819	-1.4108	-1.4112
10	-4.3698	-4.1406	-4.1492
20	-6.1798	-5.3958	-5.4662
30	-7.5687	-7.7976	-7.8025
40	-8.7396	-9.7516	-9.8346
50	-9.7712	-9.1585	-9.1857
60	-10.704	-13.736	-14.344
70	-11.561	-13.209	-13.375
80	-12.36	-12.26	-12.26
90	-13.109	-12.103	-12.158

Table 9

The table 10 offers insights into the performance of two different approximation methods in comparison to an exact formula over varying intervals of time. At first glance, it is evident that both approximation methods initially track closely with the exact formula. However, as horizon of the VaR calculation increases, disparities emerge, with both methods consistently underestimating the true values. The Delta Approximation method shows a gradual divergence from the exact formula. While it starts relatively close, its values consistently fall below those of the exact formula, with increasingly negative deltas as time advances. Similarly, the Delta Gamma Approximation method follows a comparable trajectory, albeit with more pronounced underestimation. One plausible explanation for these discrepancies could be the inherent complexity of the function being approximated. As the horizon extends, the behaviour of the bond price with respect to YTM may become more intricate, challenging the approximation methods to accurately capture its nuances. Moreover, Delta Gamma Approximation incorporates additional refinements compared to the simpler Delta Approximation, leading to more pronounced deviations over time. Furthermore, these results underscore the importance of ongoing model refinement and validation. Continuous improvement of approximation methods is essential to enhance their accuracy and reliability, particularly over extended time frames.

Additionally, to improve accuracy Monte Carlo Simulations (MCS) can be applied to the above-mentioned methods. The procedure begins by simulating variations in YTM values for bonds using a normal distribution with mean zero and standard deviation of 0.006. Then adding the simulated variations to the above computed YTM of 3.22% in order to further simulate 100000 bond prices which are calculated based on the present value formula. After obtaining simulated bond prices, the analysis focuses on estimating Value at Risk (VaR) through three distinct Monte Carlo methods: Full Revaluation, Delta Approximation & Delta-Gamma Approximation, which yielded the results below:

Days	Full Revaluation MC	Delta Approximation MC	Delta Gamma Approximation MC
1	-1.3825	-1.3819	-1.3826
10	-4.3817	-4.3768	-4.3985
20	-6.1817	-6.2239	-6.2776
30	-7.5465	-7.6672	-7.7582
40	-8.6838	-8.9036	-9.0347
50	-9.6709	-10.014	-10.19
60	-10.558	-11.028	-11.25
70	-11.362	-11.977	-12.251
80	-12.111	-12.864	-13.192
90	-12.804	-13.711	-14.096

Table 10

Firstly, the Full Revaluation Monte Carlo method directly simulates bond prices and derives VaR from the resulting distribution of simulated prices. This approach provides comprehensive VaR estimates by considering the complete distribution of bond prices. However, it demands substantial computational resources due to its exhaustive simulation process. Secondly, the Delta Approximation Monte Carlo method estimates VaR by approximating the change in bond price concerning variations in yield (delta). While computationally more efficient compared to Full Revaluation, this method may introduce slight inaccuracies due to its simplifications in estimating the bond price changes.

Lastly, the Delta-Gamma Approximation Monte Carlo method further refines VaR estimation by incorporating both delta and gamma, representing the second derivative of bond price concerning changes in yield. This method aims to enhance accuracy by considering additional factors influencing bond prices. However, it comes at the cost of increased computational complexity compared to the Delta Approximation. Ultimately, the choice of VaR estimation method hinges on the specific requirements and constraints of the risk management scenario. While Full Revaluation offers the most accurate VaR estimates, it may not always be feasible due to computational demands. Conversely, the Delta and Delta-Gamma Approximation methods provide computational efficiency but may sacrifice some level of accuracy.

Therefore, practitioners must carefully weigh the trade-offs between accuracy and computational efficiency when selecting an appropriate VaR estimation method for their risk management needs.

From table 11 one can deduce across all three simulation methods, a consistent trend emerges: VaR estimates increase as the time horizon extends. This trend underscores a fundamental principle in finance – the longer the investment period, the greater the inherent risk. This observation aligns with common intuition and financial theory, as extended time horizons expose bonds to a wider array of market fluctuations and uncertainties like changes in yields. When comparing the VaR estimates obtained from different simulation techniques, distinct patterns emerge. The Full Revaluation method, which provides a comprehensive and accurate assessment by recalculating the portfolio's value at each time step, generates relatively conservative VaR estimates. Conversely, the Delta Approximation method tends to yield slightly higher VaR estimates compared to Full Revaluation, suggesting a trade-off between computational speed and accuracy. The Delta Gamma Approximation method introduces additional complexity by incorporating second-order derivatives (gamma) alongside delta. This inclusion accounts for curvature effects in the bond's value function, resulting in the most conservative VaR estimates among the three techniques. This method provides a more nuanced understanding of risk dynamics, particularly in scenarios where nonlinearities play a significant role. Overall, the table 2 once again underscores the importance of balancing computational efficiency with accuracy in quantitative risk assessment, highlighting the nuanced trade-offs inherent in financial modelling and analysis.

While VaR is extensively used in the financial literature it is important to note that VaR is not a coherent risk measure. The primary criticism against VaR stems from its treatment of tail risk – the potential for extreme events to cause significant losses. VaR tends to focus on the most probable outcomes and often overlooks these tail events, which can have devastating consequences during periods of market stress or volatility. As a result, the sum of individual VaR estimates may underestimate the true risk exposure of the entire portfolio. This failure to account for tail risk. the coherence of VaR as a risk measure, as it leads to a misrepresentation of the overall risk. For risk measure to be coherent it must satisfy the following four properties: Monotonicity, Positive Homogeneity, Sub-Additivity and Translation Invariance. Monotonicity is a fundamental characteristic of coherent risk measures, stating that higher levels of risk should correspond to higher measures of risk. In other words, if one portfolio has more risk exposure than another, its risk measure should yield a higher value. This property aligns with the intuitive understanding that increased exposure to risk should result in a higher level of concern. Positive homogeneity implies that if the size of a position or portfolio is multiplied by a positive scalar, the risk measure of the scaled position should also be multiplied by the same scalar. Put simply, positive homogeneity states that doubling the size of a position should result in a doubling of the risk measure. Sub-additivity states that the risk measure of a combined portfolio should be less than or equal to the sum of the risk measures of its individual components. In essence, diversifying across multiple assets or positions should reduce overall risk exposure, leading to a lower aggregate risk measure. Sub-additivity reflects the benefits of portfolio diversification in reducing the impact of individual risks. Translation invariance postulates that adding or subtracting a constant value from a portfolio's wealth should not alter its risk measure. Essentially, risk assessment should be independent of the absolute level of wealth or position size. Hence using a coherent risk measure like the conditional VaR (CVaR) also known as Expected Shortfall (ES) is useful in the case of extreme events.

ES quantifies the average magnitude of losses beyond the VaR threshold, providing a more comprehensive measure of tail risk. Unlike VaR, which only considers the likelihood of extreme losses, ES captures the severity of such losses, offering a more nuanced understanding of portfolio risk. ES's coherence ensures that the aggregated risk of a portfolio accurately reflects the sum of the risks of its individual components, even in the presence of tail risk. By accounting for the entire distribution of losses beyond the VaR level, ES offers a more robust assessment of portfolio risk, particularly during turbulent market conditions.

For the purpose of comparison, the ES values for the bond were also computed using the parametric approach. This consists of the following ES formula:

$$ES_{\alpha}^t = \frac{\phi(\Phi^{-1}(\alpha)) \times \sigma_{dy} \times \sqrt{t} \times P0}{1 - \alpha}$$

where  $\phi$  = pdf of Gaussian distribution

This yielded the following results:

Days	VaR	ES
1	-1.3819	-1.5831
10	-4.3698	-5.0063
20	-6.1798	-7.08
30	-7.5687	-8.6712
40	-8.7396	-10.013
50	-9.7712	-11.194
60	-10.704	-12.263
70	-11.561	-13.245
80	-12.36	-14.16
90	-13.109	-15.019

Table 11

Firstly, there is a discernible pattern of increasing risk as the time horizon extends. Both VaR and ES exhibit a consistent upward trend, indicating that the longer the investment period, the higher the potential for loss. This aligns with conventional wisdom in finance, which recognizes that longer time horizons inherently entail greater uncertainty and exposure to market fluctuations.

A notable distinction between VaR and ES is evident throughout the results. While both measures demonstrate similar increasing trends, ES consistently yields higher estimates compared to VaR. This discrepancy arises from the fundamental differences in their calculation methodologies. VaR provides an estimate of the maximum potential loss at a specified confidence level, while ES goes a step further by quantifying the average magnitude of losses beyond the VaR threshold. Consequently, ES inherently incorporates tail risk, capturing the potential severity of losses in extreme scenarios.

The widening gap between VaR and ES as the time horizon increases underscores the growing importance of tail risk over longer periods. ES, by accounting for the average magnitude of losses beyond the VaR threshold, offers a more nuanced understanding of the portfolio's risk profile. This is particularly valuable in scenarios characterized by extreme market conditions or outlier events, where traditional risk measures like VaR may fall short in capturing the true extent of potential losses.

All the above computations for VaR and ES were done assuming a parametric approach i.e. the variations in the yields follow a Gaussian distribution. It is more dependable for shorter horizon estimation than for longer horizons. Over longer horizons the assumption of yields being normally distributed break downs since there is a higher probability that the daily volatility changes significantly from 0.6%. This implies for a longer horizon the model will fail to capture extreme events in the tails accurately. Hence using the VaR and ES estimates for longer horizons is not advisable. This method come with inherent drawbacks, including historical dependence, model dependency, and limited ability to capture extreme events. Such shortcomings have led to the emergence of non-parametric approaches, which offer an alternative methodology for VaR estimation.

Non-parametric VaR calculation stands out for its simplicity and flexibility, as it does not rely on assumptions about the underlying distribution of returns. Instead, it directly utilizes historical return data to determine VaR, making it particularly well-suited for financial markets where returns may exhibit non-normal behaviours such as skewness or heavy tails. By ranking historical returns and selecting the appropriate percentile, non-parametric VaR provides a measure of risk based solely on empirical observations, thereby mitigating concerns associated with model dependency and limited capture of extreme events.

Despite its advantages, non-parametric VaR estimation faces several challenges. Data intensity poses a significant hurdle, as reliable estimates often require a large amount of data, which may not always be available or representative of future conditions. Historical bias is another concern, as the approach assumes that past patterns will continue into the future, potentially overlooking shifts in market dynamics.

Moreover, computational complexity and the dimensionality problem can limit the scalability of non-parametric methods, particularly in high-dimensional datasets or scenarios involving complex dependencies. Therefore, in practice it is best to use the combination of both methods, parametric and non-parametric i.e. semi-parametric approach. One way of using semi-parametric method is as follows: for shorter horizons model VaR estimates via assuming the variations in yield are Gaussian distributed and for longer horizons estimate VaR by directly sampling from the Empirical CDF of the variations in yield.

## 4.1 References

- Christoffersen, P 2003, Elements of Financial Risk Management, Elsevier Science & Technology, San Diego.
- Britten-Jones, M., and Schaefer S. M. (1999). Non-Linear Value-at-Risk, European Finance Review 2: 161–187, 1999.
- Capriotti, L. and M. Giles (2010) Fast Correlation Greeks by Adjoint Algorithmic Differentiation, Risk Magazine, April.
- Cardenas, J., E. Fruchard, J.-F. Picon, C. Reyes, K. Walters, and W. Yang (1999) Monte Carlo within a day. Risk Magazine 12 (February): 55-59.
- Glasserman P. (2003) Monte Carlo Methods in Financial Engineering Springer-Verlag, New York.
- Giles m., and Glasserman, P., (2006) Smoking adjoints: fast Monte Carlo Greeks, Risk Magazine 19 (January), 92-96.
- Rouvinez, C. (1997) Going Greek with VaR. Risk 10 (February): 57-65.
- Jorion, P. (2007) Value at Risk, 3<sup>rd</sup> ed.